INL/CON-23-72076-Revision-0

Severe Temperature Impact Study on Ferrite Electromagnetic Shielding for Wireless Electric Vehicle Charging

July 2023

Bo Zhang, Yukiyasu Yamauchi, Veda P. Galigekere, Omer C. Onar, Mostak Mohammad

Changing the World's Energy Future

INL is a U.S. Department of Energy National Laboratory operated by Battelle Energy Alliance, LLC

INL/CON-23-72076-Revision-0

Severe Temperature Impact Study on Ferrite Electromagnetic Shielding for Wireless Electric Vehicle Charging

Bo Zhang, Yukiyasu Yamauchi, Veda P. Galigekere, Omer C. Onar, Mostak Mohammad

July 2023

Idaho National Laboratory
Idaho Falls, Idaho 83415

http://www.inl.gov

Prepared for the
U.S. Department of Energy
Under DOE Idaho Operations Office
Contract DE-AC07-05ID14517

Severe Temperature Impact Study on Ferrite Electromagnetic Shielding for Wireless Electric Vehicle Charging

Bo Zhang
Department of Energy Storage and Electric Transportation
Idaho National Laboratory
Idaho Falls, ID USA
bo.zhang@inl.gov

Yukiyasu Yamauchi
KEMET Electronics
Milpitas, CA USA
Yukiyasu.yamauchi@yageo.com

Veda P. Galigekere
National Transportation Research Center
Oak Ridge National Laboratory
Knoxville, TN USA
galigekerevn@ornl.gov

Omer C. Onar
National Transportation Research Center
Oak Ridge National Laboratory
Knoxville, TN USA
onaroc@ornl.gov

Mostak Mohammad
National Transportation Research Center
Oak Ridge National Laboratory
Knoxville, TN USA
mohammadm@ornl.gov

***Abstract*— Wireless charging of an electric vehicle (EV) is an emerging technology that enables noncontact charging, which has advantages in terms of convenience and flexibility. However, the embedded charging pads under and on the ground expose the charging coils, ferrite shielding, and related components to a potentially severe external environment. To study the electromagnetic shielding performance under such extreme temperature conditions, ferrite shielding material's permeability characteristics are tested under temperatures as low as -50°C to as high as 240°C. Referring to the official recorded lowest and highest temperature of the United States, in this paper, it is assumed that the operation temperature ranges from -50°C to 57°C as the coldest winter and hottest summer environment for WPT application. Electromagnetic performance, shielding, and associated stray magnetic emissions are simulated by using three-dimensional (3D) transient simulations to study the impact of low and high temperature on electromagnetic shielding performance. Based on ferrite testing data, from -50°C low temperature to 57°C high temperature, the ferrite's relative permeability ranges from 2550 to 3727. The simulation study indicates that there won't be significant impact on the EM shielding performance for WPT operated under those severe environment temperature conditions.**

Keywords—wireless power transfer, inductive power transfer, electric vehicle, electromagnetic field, ferrite shielding.

I. Introduction

Wireless power transfer (WPT) is a noncontact, convenient electric vehicle (EV) charging technology [1-4]. Some electromagnetic (EM) shielding solutions have been developed for stationary and 200-kW dynamic wireless charging of light-duty electric vehicles (LDEVs) [5-8]. However, the embedded charging pads under and on the ground expose the charging coils and ferrite shielding to a potentially severe external cold or hot environment. As such, EM shielding performance under such conditions need further study.

Most of the publications in the WPT field focus on power electronics control or interoperability studies [9-14]. In terms of charging pads and EM analysis, three-dimensional (3D) coil positioning of EM coupling is studied in Gao et al. [15]. Control strategies to improve the magnetic coupling and mitigate stray EM fields are presented in Lin, Covic, and Boys [16]. Tavakoli et al. [17] compared the EM coupling of different lumped and shaped pads/rails for cost optimization. These methodologies are great solutions to increase the EM coupling and mitigate stray EM emissions, but few methodologies focus on the shielding material's characteristic study under an extreme low- and high-temperature environment.

This paper investigates the permeability characteristics of ferrite shielding material and its impact on EM WPT field emissions. The permeability of ferrite samples was tested at an extreme temperature range of -50°C to 240°C. Stray magnetic emissions are simulated using 3D transient simulations to study the impact of low- and high-temperature in the range of -50°C to 57°C on the performance of electromagnetic shielding. In this paper, the analysis focuses on in-motion dynamic wireless power transfer (dWPT) as an example to conduct simulation; however, low- and high-temperature impact on EM performance is applicable to both dWPT and static WPT.

II. Wireless Charging Scenario and Charging Pards in/on the Ground

In the electrified lane, high-power wireless charging pads are installed on a roadway. When LDEVs pass by, ground-side wireless pads are energized alternatively to charge the in-motion EVs. EM coupling factor between the vehicle and charging pad

This manuscript was authored by Idaho National Laboratory, operated by Battelle Energy Alliance with the U.S. Department of Energy under DOE Contract No. DE-AC07-05ID14517. This manuscript has been co-authored by Oak Ridge National Laboratory, operated by UT-Battelle, LLC, under Contract No. DE-AC05-00OR22725 with the U.S. Department of Energy. The United States Government retains and the publisher, by accepting the article for publication, acknowledges that the United States Government retains a nonexclusive, paid-up, irrevocable, worldwide license to publish or reproduce the published form of this manuscript, or allow others to do so, for United States Government purposes. The Department of Energy will provide public access to these results of federally sponsored research in accordance with the DOE Public Access Plan (http://energy.gov/downloads/doe-public-access-plan).

is a key parameter determining the dWPT charging effectiveness. For dWPT, assuming that the coils' resistances are negligible compared to coils' inductances or load battery impedance, the output power P_0 of dWPT can be written as follows:

$$P_0 = v_v i_v = \omega M I_g I_v sin\varphi_{gv} \quad (1)$$

where v_v and i_v present the transient vehicle-side voltage and current, respectively; I_g and I_v are the RMS values of the ground- and vehicle-side currents, respectively. M is the mutual inductance between the ground- and vehicle-side coils, and $sin\varphi_{gv}$ is the power factor on the vehicle-side. The mutual inductance M is given by the following:

$$M = k\sqrt{L_g L_v} \quad (2)$$

where k is the coupling coefficient typically between 0.1 and 0.5, owing to the loose coupling [18]. L_g and L_v present the ground-side and vehicle-side coil self-inductance.

The electromagnetic field coupling contributes to the power transfer, but a downside to the coupling is the stray EM field emission could be a safety concern for human health. The Society of Automotive Engineers (SAE) standard J2954 defines a maximum allowable magnetic field of 27 μT at 0.8 m (derived from a typical LDEV width of 1.6 m) from the center of the vehicle-side coil for LDEV stationary WPT [19], as shown in Fig. 1, but no dWPT standard exists yet.

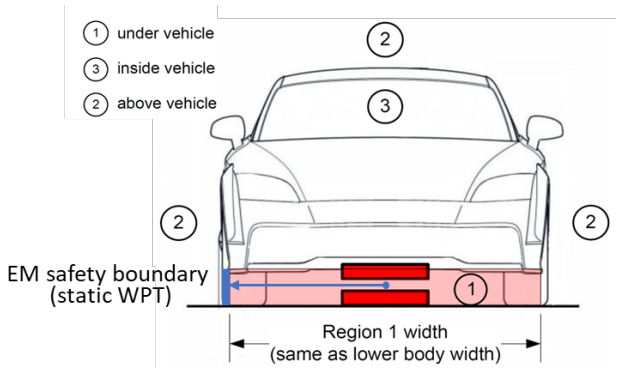

Fig. 1. EM safety boundary for static WPT [19].

As the wireless charging pads are installed along the roadway, they are exposed to the external environment such as cold temperatures in the winter or hot temperatures in the summer, as shown in Fig. 2. Additionally, the charging pads installed under the ground are exposed to a high-temperature environment and experience a lack of air flow or heat exchange circumstance, which causes an accumulated effect that could be even worse when fault current occurs on the underground charging pads. To ensure safety, EM performance under those extreme temperature conditions should be studied.

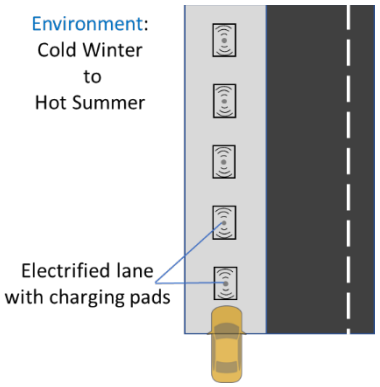

Fig. 2. Typical dWPT scenarios with wireless charging pads installed along the electrified roadway.

III. Permeability-Temperature Characteristic Tests of Ferrite Material

As a high-permeability material, ferrite is widely used as a shielding component for high-power WPT and dWPT prototypes [6]. Because the charging pads might be exposed to a high- and low-temperature environment, it is vital to study the EM characteristics of the ferrite material under extreme temperature conditions to ensure proper operation.

A. Measurement Method

To obtain the relative permeability-temperature curve, the permeability of a ferrite sample (BH1T, KEMET) has been tested at the ferrite test facility at temperatures ranging from -50°C to 240°C. Table 1 presents the parameters of the tested samples and test condition.

TABLE I. Ferrite Test Parameters

Quantity	Value [unit]
Test ferrite piece size	25 x 15 x 10 [mm]
Frequency	100 [kHz]
Current	0.1 [mA]
Measured performance	inductance
Associated windings	Φ0.26 [mm] x 10 [turns]
Temperature	-50 to 240 [degC]

For a test setup with winding and ferrite core, assuming the ferrite permeability is not saturated when magnetic field is low, the permeability μ_r can be calculated as such:

$$\mu_r = \left(\frac{Ll}{4\pi AN^2}\right) \times 10^7 \quad (3)$$

where μ_r is the relative permeability. L is the measured inductance (H), l is the average magnetic path length (m), A is the cross-section area (m^2), and N is the number of the associated winding turns. Fig. 3 demonstrates the measurement circuit setup.

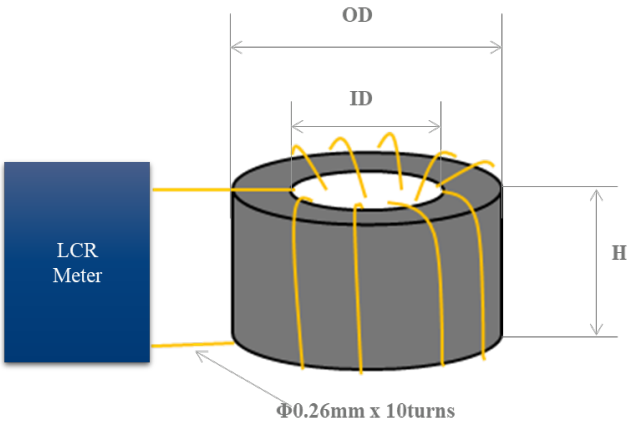

Fig. 3. Measurement circuit setup for relative permeability test.

B. Measure Equipment

(a)

(b)

Fig. 4. Measurement equipment at KEMET facility [20]: (a) LCR meter and thermostatic chamber for -50 to 100°C; (b) LCR meter and thermostatic chamber for 100 to 300°C.

The measurement equipment is present, as depicted in Fig. 4. The FL721N-E type thermostatic chamber from Maker ETAC is used to carry out permeability test from -50 to 100°C, as shown in Fig. 4 (a), while HPS-222 type thermostatic chamber from Maker TABAI is used to carry out high-temperature test from 100–300°C, as shown in Fig. 4 (b).

C. Measured Result

Fig. 5 presents the results of the relative permeability-temperature characteristics of the ferrite material test.

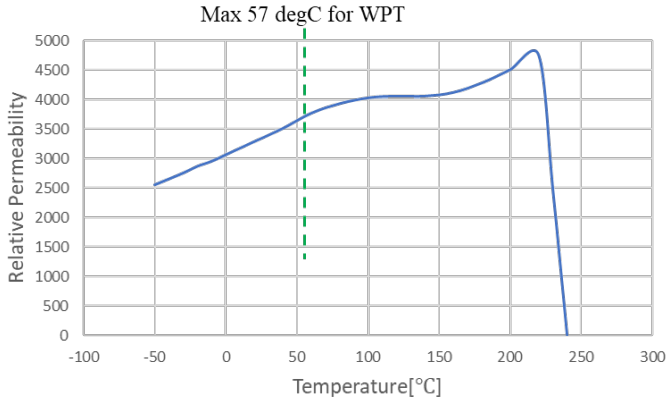

Fig. 5. Results of the relative permeability-temperature characteristics of ferrite material test.

According to the tested data shown in Fig. 5, the ferrite's relative permeability declines from 3074 to 2550, with the temperature dropping from 0°C to -50°C. Historically, the lowest official, minimum recorded temperature of the contiguous United States was -56.7°C in Montana on January 20, 1954 [21]. Normally, it is very rare to have environment temperatures drop below -50°C [21]. In this paper, considering -50 °C as the theoretically lowest temperature for dWPT operation, the ferrite's relative permeability drops from 3074 to 2550.

On the high temperature end, the relative permeability of the ferrite drops significantly when the temperature climbs over 220°C. It quickly reduces to 1 (no shielding effectiveness) when approaching 240°C. However, normal environment temperature even in the hottest summer ever won't be as high as 220°C. Historically, the highest recorded official temperature of the United States was 134 degrees Fahrenheit or 56.7°C, which occurred at Greenland Ranch in Death Valley, California on July 10, 1913 [22]. No other United States location has ever come close to this historical hot summer. Considering 57 °C as the theoretically highest environment temperature for dWPT operation as the worst-case scenario, the ferrite's relative permeability increases from 3074 to 3727, and it is still under the ferrite deficiency point of 220°C by a considerable margin.

IV. Simulation Studies of Temperature Impact on Shielding Performance

A 200-kW dWPT system with parameters referring to Zhang, et al. [6] is presented as an example on how to conduct the analysis. The finite-element model of both the ground-side and vehicle-side couplers are shown in Fig. 6, where both the ground-side coil/shielding and the vehicle-side coil/shielding are modeled in detail.

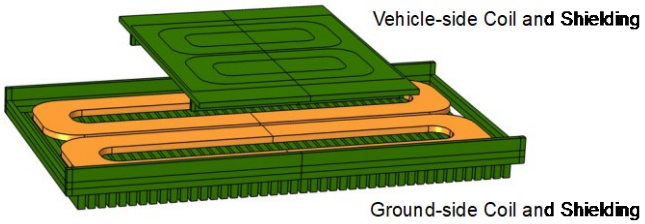

Fig. 6. 3D transient finite-element simulation model for EM emission analysis.

To represent the in-motion charging scenario, previously shown in Fig. 2, symmetric boundaries along the driving direction are adopted to enable multiple ground-side charging pads considered in transient simulation computing. Fig. 7 presents the transient model setup when EV is aligned with ground-side coils. To mimic multiple ground-side coils along the electrified lane, the symmetric boundary with magnetic field B, which is set in parallel with symmetric boundary, is utilized to ensure symmetric magnetic field distribution along the electrified lane.

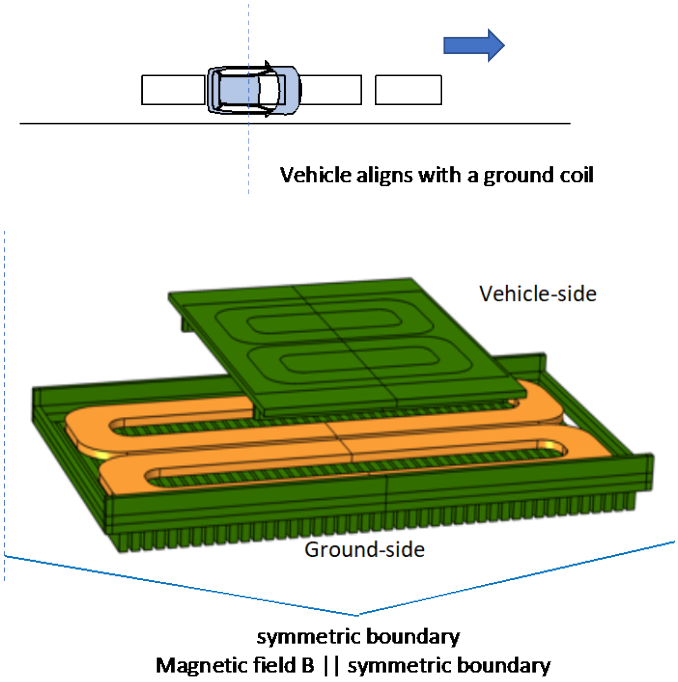

Fig. 7. 3D transient finite-element simulation model for EM emission analysis.

Fig. 8 presents the results for the EM emission simulation comparison along with a side-to-side direction under normal and cold weather operation conditions. The simulation model is preliminarily verified in static mutual-inductance measurement in Zhang, et al. [6]. According to the results shown in Fig. 8, when the environment temperature drops from 0°C to -50°C, there is only a slight stray field increase in EM field emissions, as shown by the green line as compared to the blue one in Fig. 8.

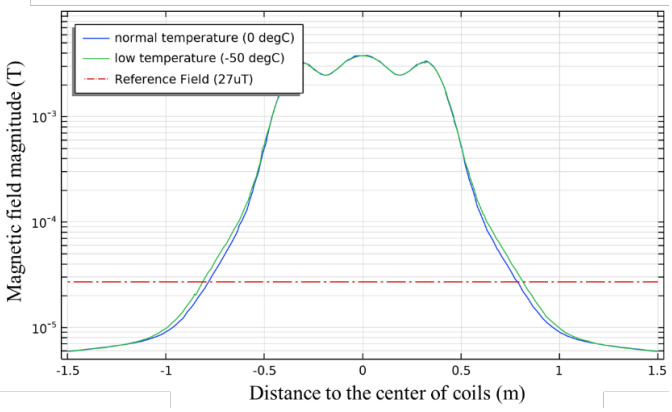

Fig. 8. Magnetic field emission comparison between normal temperature and -50°C low temperature.

On the high-temperature end, on the contrary, the EM shielding performance even improves a bit. Fig. 9 presents the results of the simulation comparison between normal and 57 °C operating conditions. According to the results shown in Fig. 9, when the temperature approaches 57 °C, the EM field emission slight decreases, as shown by the green line as compared to the blue one. This is because the ferrite material's relative permeability, as shown in Fig. 5, increases to 3727 when the temperature increases to 57 °C compared to the relative permeability of 3074 in 0 °C.

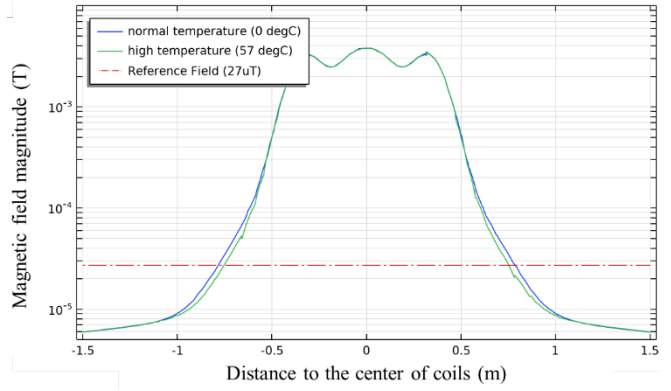

Fig. 9. Magnetic field emission comparison between normal temperature and 57 °C high temperature.

Fig. 10 demonstrates the magnetic field distribution comparison from -50 °C to +57 °C. It is observed that under the typical operation conditions with temperature ranging from as low as -50°C in the cold winter up to 57 °C in the hot summer, there won't be significant EM performance degradation. Lower temperature leads to slightly weaker EM field centralization as show in Fig. 10 (a), thus a bit higher EM field emission as shown in Fig. 8. But in general, the temperature in the range of -50 °C to +57 °C doesn't have significantly negative impact on the EM performance.

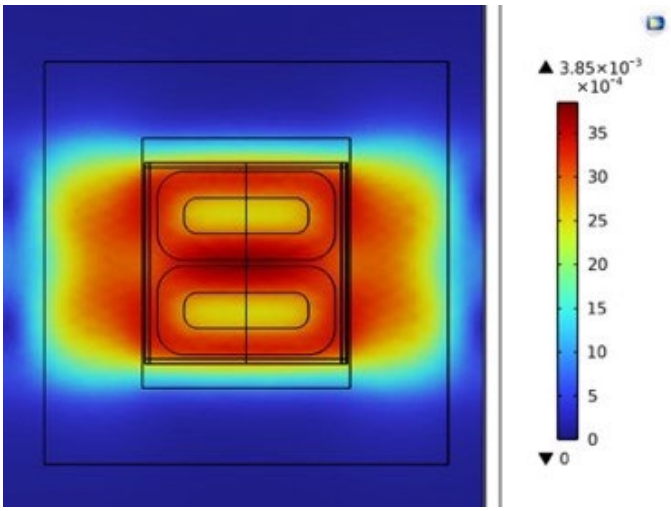

(a)

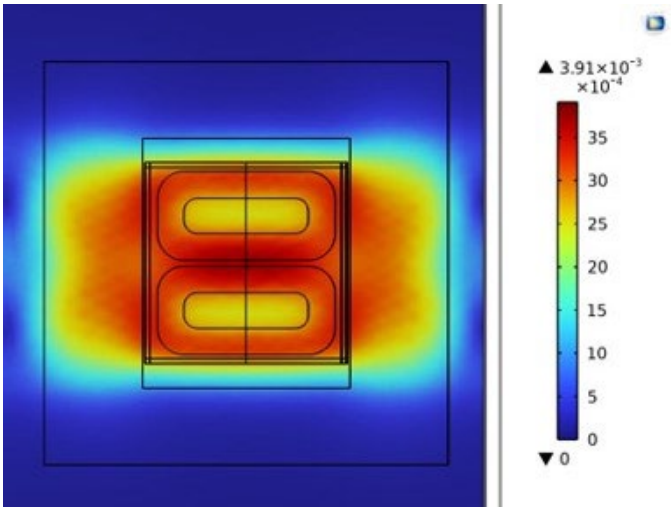

(b)

Fig. 10. Magnetic field distribution when (a) -50 °C in the winter and (b) 57 °C in the summer.

V. Conclusion and Discussion

This paper presents the permeability test curve of the ferrite shielding material and its impact simulation on EM field emissions for WPT. The test methods, equipment, and conditions are presented in detail. The permeability of the ferrite samples is tested from -50°C to 240°C, where the relative permeability of the ferrite drops significantly when the temperature climbs over 220°C, and quickly reduces to 1 when approaching 240°C. Referring to the official lowest and highest recorded temperature of the United States, 220°C is unrealistic, thus in this paper, it is assumed that the operation temperature ranges from -50°C to 57°C as the coldest winter and hottest summer environment for WPT application.

Based on the tested ferrite permeability curve, from -50°C low temperature to 57°C high temperature, the ferrite's relative permeability ranges from 2550 to 3727. A stray magnetic emission is simulated using 3D transient simulations to study the impact of low and high temperatures on electromagnetic shielding performance. The simulation study indicates that there won't be significant impact on the EM shielding performance for WPT operated under those severe environment temperature conditions. Currently, the full-size, high-power dWPT has been tested functionally at Oak Ridge National Laboratory (ORNL). The hardware deployment and integration with real world roadway conditions is in under coordination and will be presented in future work.

Acknowledgment

This work was supported by the U.S. Department of Energy (DOE), Vehicle Technologies Office, under the project FY2022 VTO: "EV@Scale- Wireless Pillar," with collaborative partners Oak Ridge National Laboratory (ORNL), Idaho National Laboratory, and National Renewable Energy Laboratory. All authors thank Lee Slezak from U.S. DOE for project oversight and technical leadership.

References

[1] C. T. Rim and C. Mi, Wireless power transfer for electric vehicles and mobile devices, John Wiley & Sons, 2017.

[2] D. Patil, M. Mcdonough, J. Miller, B. Fahimi, and P. Balsara, "Wireless Power Transfer for Vehicular Applications: Overview and Challenges," IEEE Transactions on Transportation Electrification, vol. 4, pp. 3–37, March 2018. (https://doi.org/10.1109/TTE.2017.2780627)

[3] Z. Zhang, H. Pang, A. Georgiadis, and C. Cecati, "Wireless Power Transfer-An Overview," IEEE Transactions on Industrial Electronics, vol. 66, pp. 1044–1058, February 2019. (https://doi.org/10.1109/TIE.2018.2835378)

[4] H. Feng, R. Tavakoli, O. Onar, and Z. Pantic, "Advances in High-Power Wireless Charging Systems: Overview and Design Considerations," IEEE Transactions on Transportation Electrification, vol. 6, pp. 886–919, September 2020.(https://doi.org/10.1109/TTE.2020.3012543)

[5] B. Zhang, R. B. Carlson, V. P. Galigekere, O. C. Onar, and J. L. Pries, "Electromagnetic Shielding Design for 200 kW Stationary Wireless Charging of Light-Duty EV," 2020 IEEE Energy Conversion Congress and Exposition (ECCE), October 2020, pp. 5185–5192. (https://doi.org/10.1109/ECCE44975.2020.9235329)

[6] B. Zhang et al., "Quasi-Dynamic Electromagnetic Field Safety Analysis and Mitigation for High-Power Dynamic Wireless Charging of Electric Vehicles," 2021 IEEE Transportation Electrification Conference & Expo (ITEC), June 2021, pp. 1–7. (https://doi.org/10.1109/ITEC51675.2021.9490192)

[7] B. Zhang, R. B. Carlson, J. G. Smart, E. J. Dufek, and B. Liaw, "Challenges of Future High Power Wireless Power Transfer for Light-duty Electric Vehicles—Technology and Risk Management," eTransportation, vol. 2, p. 100012, 2019.(https://doi.org/10.1016/j.etran.2019.100012)

[8] B. Zhang et al., "Concept Design of Active Shielding for Dynamic Wireless Charging of Light-duty EV," 2020 IEEE Transportation Electrification Conference & Expo (ITEC), June 2020, pp. 844–850. (https://doi.org/10.1109/ITEC48692.2020.9161606)

[9] A. Ahmad, M. S. Alam, and A. A. S. Mohamed, "Design and Interoperability Analysis of Quadruple Pad Structure for Electric Vehicle Wireless Charging Application," IEEE Transactions on Transportation Electrification, pp. 1, 2019. (https://doi.org/10.1109/TTE.2019.2929443)

[10] L. Zhao, D. Thrimawithana, U. Madawala, A. Hu, and C. Mi, "A Misalignment-Tolerant Series-Hybrid Wireless EV Charging System With Integrated Magnetics," IEEE Transactions on Power Electronics, vol. 34, pp. 1276–1285, February 2019. (https://doi.org/10.1109/TPEL.2018.2828841)

[11] M. Mohammad, S. Choi, M. Islam, S. Kwak, and J. Baek, "Core Design and Optimization for Better Misalignment Tolerance and Higher Range of Wireless Charging of PHEV," IEEE Transactions on Transportation

Electrification, vol. 3, pp. 445–453, June 2017. (https://doi.org/10.1109/TTE.2017.2663662)

[12] C. Zhang, S. Srdic, S. Lukic, Y. Kang, E. Choi, and E. Tafti, "A SiC-Based 100 kW High-Power-Density (34 kW/L) Electric Vehicle Traction Inverter," 2018 IEEE Energy Conversion Congress and Exposition (ECCE), 23-27 September 2018, pp. 3880–3885. (https://doi.org/10.1109/ECCE.2018.8558373)

[13] T. Kan, F. Lu, T. Nguyen, P. P. Mercier, and C. C. Mi, "Integrated Coil Design for EV Wireless Charging Systems Using LCC Compensation Topology," IEEE Transactions on Power Electronics, vol. 33, pp. 9231–9241, 2018. (https://doi.org/10.1109/TPEL.2018.2794448)

[14] T. Yilmaz, N. Hasan, R. Zane, and Z. Pantic, "Multi-Objective Optimization of Circular Magnetic Couplers for Wireless Power Transfer Applications," IEEE Transactions on Magnetics, vol. 53, August 2017, vol. 58. (https://doi.org/10.1109/TMAG.2017.2692218)

[15] Y. Gao, C. Duan, A. Oliveira, A. Ginart, K. Farley, and Z. Tse, "3-D Coil Positioning Based on Magnetic Sensing for Wireless EV Charging," IEEE Transactions on Transportation Electrification, vol. 3, pp. 578–588, September 2017. (https://doi.org/10.1109/TTE.2017.2696787)

[16] F. Lin, G. Covic, and J. Boys, "Leakage Flux Control of Mismatched IPT Systems," IEEE Transactions on Transportation Electrification, vol. 3, pp. 474–487, June 2017. (https://doi.org/10.1109/TTE.2016.2630922)

[17] R. Tavakoli, E. M. Dede, C. Chou, and Z. Pantic, "Cost-Efficiency Optimization of Ground Assemblies for Dynamic Wireless Charging of Electric Vehicles," IEEE Transactions on Transportation Electrification, pp. 1, 2021. (https://doi.org/10.1109/TTE.2021.3105573)

[18] V. Jiwariyavej, T. Imura, and Y. Hori, "Coupling Coefficients Estimation of Wireless Power Transfer System via Magnetic Resonance Coupling Using Information From Either Side of the System," IEEE Journal of Emerging and Selected Topics in Power Electronics, vol. 3, pp. 191–200, March 2015. (https://doi.org/10.1109/JESTPE.2014.2332056)

[19] SAEJ2954. "Wireless Power Transfer for Light-Duty Plug-in/Electric Vehicles and Alignment Methodology," https://www.sae.org/standards/content/j2954_202010/. (accessed November 1, 2020).

[20] KEMET, https://www.kemet.com/en/us.html. (accessed Apr 1, 2023).

[21] L. Osborn. "Coldest Temperatures in the United States," https://www.currentresults.com/Weather-Extremes/US/coldest-temperatures.php. (accessed December 1, 2022).

[22] L. Osborn. "Hottest Temperatures in the United States," https://www.currentresults.com/Weather-Extremes/US/hottest.php. (accessed December 1, 2022).